Fabricating Continuous Supercapacitor Fibers with High Performances by Integrating All Building Materials and Steps into One Process

*Bingjie Wang, Xin Fang, Hao Sun, Sisi He, Jing Ren, Ye Zhang, and Huisheng Peng**

The popular concept of wearable electronic devices has motivated the exploration for suitable powering accessories such as flexible and portable energy conversion and storage devices.[1–3] Among them, the developing fiber-shaped energy devices are increasingly appreciated as a reliable strategy to leap over the geometrical restrictions of traditional planar devices.[4–6] In the diversified fiber-shaped energy devices, fiber-shaped supercapacitors are approaching toward macro-scale devices for wearable electronics or smart textiles.[7,8] In most cases, fiber-shaped supercapacitors are assembled from fibrous electrodes in which carbonaceous materials, including carbon fibers, carbon nanotube fibers, and graphene fibers, play a dominant role due to their merits of flexibility, lightweight, and high surface area.[9–11] Moreover, pseudocapacitive materials such as metal oxides and conducting polymers are often introduced into the fibrous electrodes to enhance the capacitance.[9,12–14]

However, these academic achievements have not yet been translated into industrial success. The pending issue resides in the fabrication process that commonly consists of four steps[9,13]—preparing the fiber substrate, introducing active materials, infiltrating the electrolyte, and assembling into a device—which notoriously entail complicated treatments and time-consuming procedures. Most currently attainable fiber-shaped supercapacitors have very limited lengths at centimeters which make them hardly applicable in wearable devices. Although many attempts have been made to realize the scale-up production of fiber-shaped supercapacitors,[8,15,16] it remains challenging to achieve a continuous fabrication.

In the present study, we design a synchronous deposition strategy to continuously fabricate fiber-shaped supercapacitors based on aligned carbon nanotube (CNT) composite fibers. This continuous fabrication strategy is available for a variety of pseudocapacitive active materials such as reduced graphene oxide (RGO), manganese dioxide (MnO_2), and conducting polymers including polyaniline (PANI) and polypyrrole (PPy), so a high energy storage capability has been produced from the fiber-shaped supercapacitor.

Our fabrication method relies on an experimental setup as illustrated in **Figure 1**. It can integrate the above four discrete fabrication steps into a continuous process. A spinnable CNT array is fastened onto a rotating motor by which CNT fibers can be produced continuously. The as-prepared CNT fiber was led to immersing into active materials solution such as graphene oxide (GO) aqueous solution. A constant potential was applied on the CNT fiber through the copper rods. Pt wire and Ag/AgCl electrode served as counter and reference electrodes, respectively. As a result, a synchronous electrochemical deposition system was established and connected with the prepared CNT fibers. During this procedure, GO sheets were coated externally on the CNT fiber and reduced to RGO, forming a core–sheath-structured CNT/RGO composite fiber. Afterward, two composite fibers were drawn into a gel electrolyte consisting of poly(vinyl alcohol) (PVA), phosphoric acid, and water, followed by twisting into a fiber-shaped supercapacitor with a rotating motor.

Our method is highlighted with several advantages: first, the entire process is continuous and spans from the preparation of CNT fiber to the fabrication of supercapacitors; second, the electrochemical method is adaptable to moving fibers which integrates the procedures of deposition, polymerization, and reduction together, which exempts from the complicated post-treatments; third, compared with previous time-consuming methods, this fabrication process can be accomplished within 5 min, demonstrating an ultrafast strategy for the scalable production of fiber supercapacitors; and fourth, GO is reduced as active material to provide pseudocapacitance instead of non-conductive GO that may cause performance degradation.[17] Yet this method is not a simple combination of individual batch processes that have been previously reported.[10] Furthermore, a new method of incorporating RGO as pseudocapacitive materials in fibrous electrodes is developed and then integrated into a continuous process through the design, which enables GO to migrate toward fibrous electrode and get reduced into RGO synchronously.

The pivotal part of the method resides in the synchronous electrochemical deposition system where the introduction of functional guest materials like graphene and pseudocapacitive materials are accomplished within several minutes. To demonstrate its efficacy, we investigated the preparation process of CNT/RGO composite fiber. When the CNT fibers with diameter of ≈20 µm were passed through the GO aqueous solution (3 mg mL^{-1}) (Figure 1b), a constant potential (between CNT fiber and Pt wire) of −1.2 V was applied on the CNT

Dr. B. Wang, X. Fang, H. Sun, S. He, J. Ren,
Y. Zhang, Prof. H. Peng
State Key Laboratory of Molecular
Engineering of Polymers
Collaborative Innovation Center of Polymers
and Polymer Composite Materials
Department of Macromolecular Science
and Laboratory of Advanced Materials
Fudan University
Shanghai 200438, China
E-mail: penghs@fudan.edu.cn

DOI: 10.1002/adma.201503441

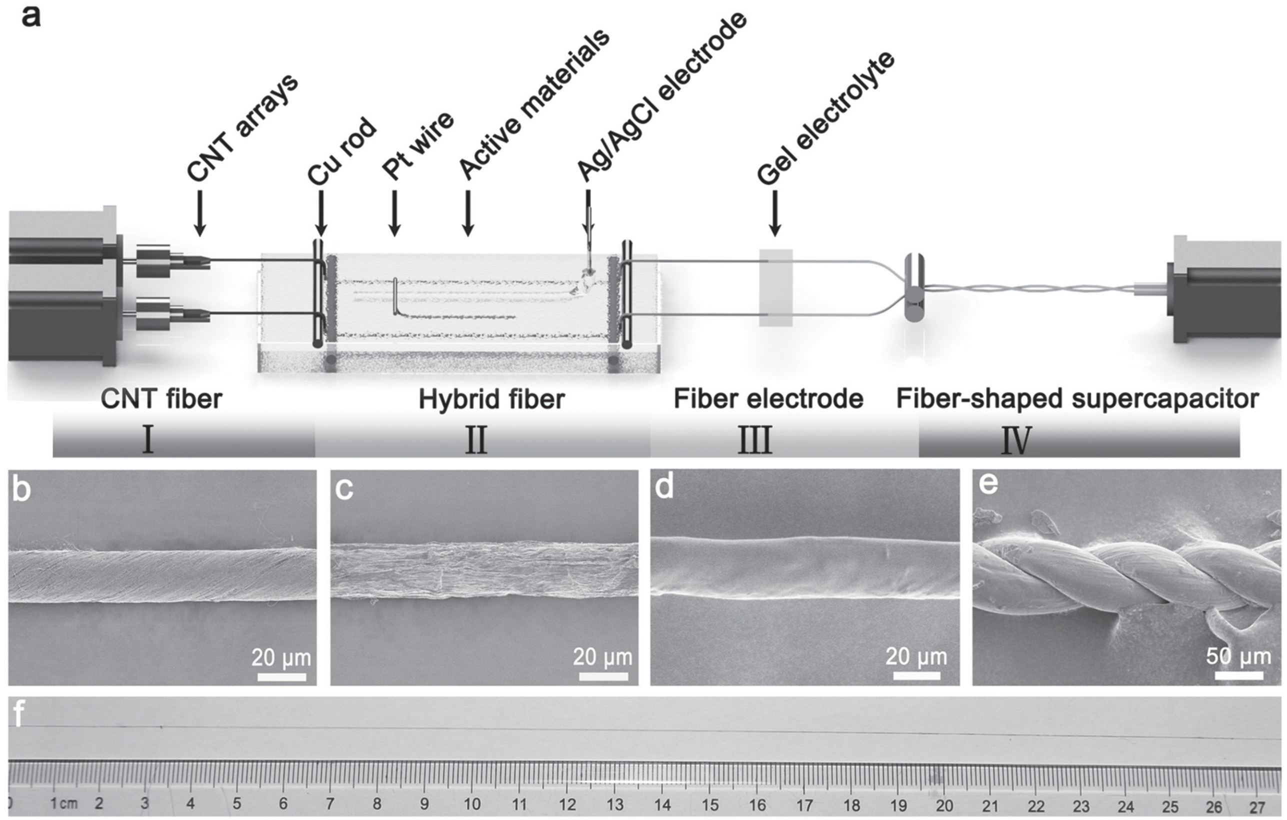

Figure 1. a) Schematic of the experimental setup for the continuous fabrication of supercapacitor fiber. b–e) SEM images of bare CNT fiber, CNT/RGO composite fiber, electrolyte-coated composite fiber, and fiber-shaped supercapacitor, respectively. f) Photograph of a continuous fiber-shaped supercapacitor with a length of ≈30 cm.

fiber through the copper rod electrode. During this process, GO sheets, usually negatively charged, were prone to migrate toward CNT fiber and synchronously reduced to RGO sheets which inclined to deposit on the surface of CNT fiber (Figure 1c and Movie S1, Supporting Information).[10]

In a typical procedure, GO was electrochemically reduced in 180 s, which was controlled by varying the drawing speed of the composite fiber. After deposition, the CNT/RGO composite fiber exhibited a typical core–sheath structure where the RGO sheets cover the CNT fiber (Figure S2, Supporting Information). Brunauer–Emmett–Teller (BET) analysis shows that RGO sheets have a specific surface area of ≈121 m^2 g^{-1} (Figure S3, Supporting Information). It was smaller than the claimed theoretical value of graphene because the strong π–π interaction makes the RGO sheets prone to stack, but the surface area is sufficient to afford a high charge storage capability. Note that a bare CNT fiber displayed a specific surface area of 160 m^2 g^{-1}.[18] The fiber continuously produced from this method had a uniform morphology and diameter, manifesting the stability of the preparation process (Figure S4, Supporting Information). The presence of CNT fiber offers the flexibility of the composite fiber, thus it can be tied into a knot without obvious structural damage (Figure S5, Supporting Information). The flexibility of the CNT/RGO composite fiber is comparable with other previously reported fiber electrodes.[10,16,19] Also, the synchronous deposition process is compatible with CNT fibers with different diameters (Figure S6, Supporting Information). Then the composite fiber was incorporated with gel electrolyte through a dip-coating process (Figure 1d). Given the surface tension and viscosity of the PVA gel, a majority of electrolyte was coated outside the composite fiber (Figure S7, Supporting Information). The thickness of electrolyte coating was 2–5 μm. The electrolyte also protects the RGO layer against fracture and prevents the short circuit between two fibrous electrodes. Twisting two fibrous electrodes, an ultralong fiber-shaped supercapacitor (up to 5 m) can be continuously fabricated, exhibiting adaptability for large-scale production (Figure 1e,f and Figure S8, Supporting Information).

The electrochemically reduced RGO layer through this method was verified by Raman spectroscopy (**Figure 2**a). For the CNT/RGO composite fiber, the intensity ratio of D to G bands was increased from 1.19 to 1.39, which was caused by more disordered graphene edges after electrochemical reduction of oxygen-containing functional groups in GO.[17,20] For systematic investigation, we prepared a series of CNT/RGO composite fibers under different deposition time. With increasing deposition time from 30 to 300 s, more RGO sheets were stacked on the surface of CNT fibers. Hence, the fiber diameters were slightly increased from 20 to 23 μm but the contents of RGO were increased from 1 to 12 wt% (Figures S9 and S10, Supporting Information).

To characterize the electrochemical performance of CNT/RGO composite fibers, we first recorded their cyclic voltammogram (CV) curves in a three-electrode electrochemical cell.

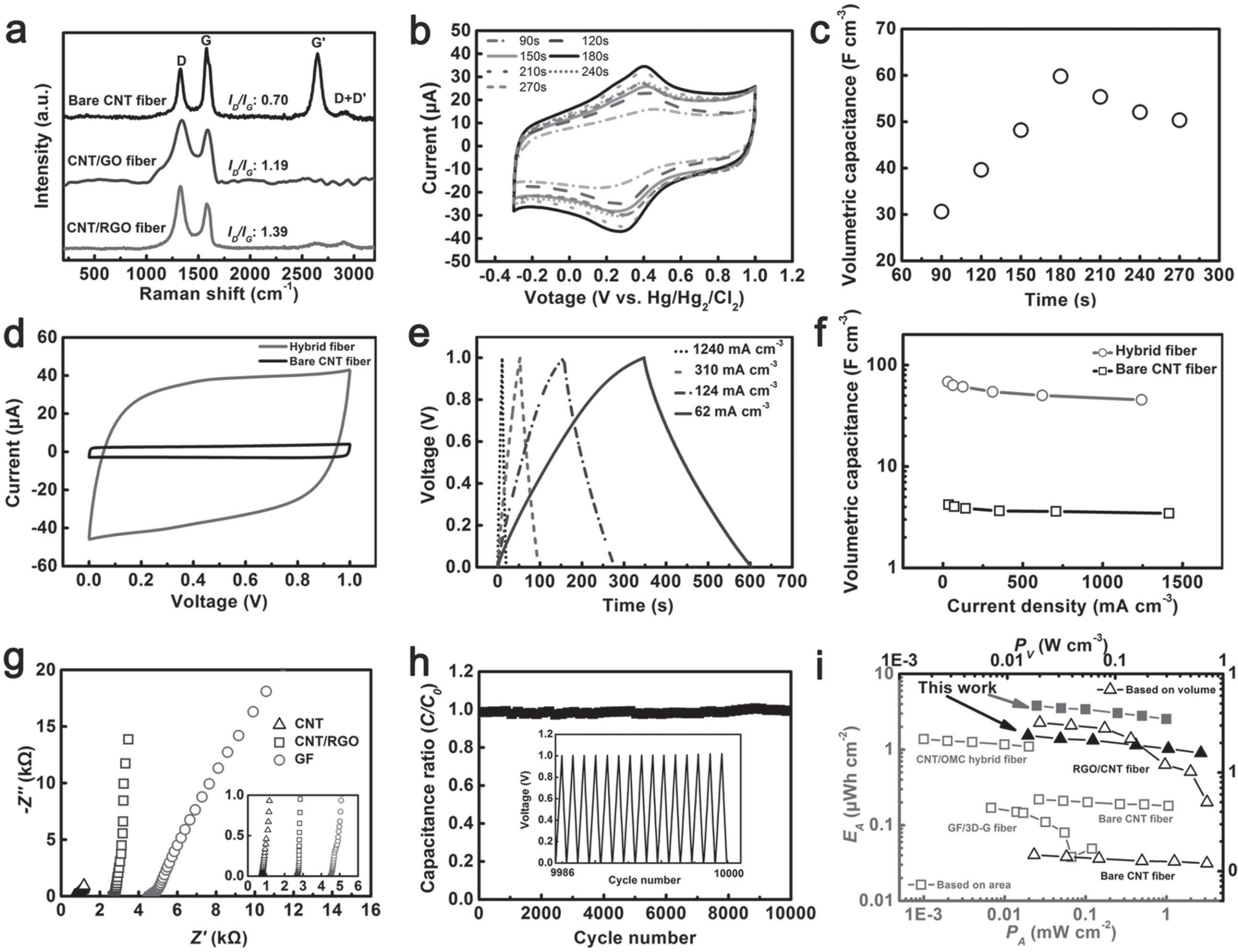

Figure 2. a) Raman spectra of CNT, CNT/GO, and CNT/RGO fibers. The deposition time for CNT/RGO composite fiber was 180 s. b) CV curves of CNT/RGO composite fibers with increasing deposition times at 50 mV s^{-1} in 1 M H_2SO_4. The CV curves were recorded in a three-electrode system where composite fiber, Pt wire, and Hg/Hg_2Cl_2 electrode were used as working, counter, and reference electrodes, respectively. c) Dependence of volumetric capacitance of the CNT/RGO composite fiber on the increasing deposition time. The discharge current density was 310 mA cm^{-3}. d) CV curves of supercapacitor fibers based on bare CNT and CNT/RGO composite fibers. The electrolyte included PVA, phosphoric acid, and water. The scan rate was 200 mV s^{-1}. e) Galvanostatic charge–discharge curves of CNT/RGO composite supercapacitor fiber at increasing current densities. f) Volumetric capacitances of supercapacitor fiber at increasing current densities. g) Electrochemical impedance spectra of supercapacitors based on different fibrous electrodes: CNT, CNT/RGO, and graphene fiber (GF). The inset is the magnified graph displaying the horizontal intercepts. Note that the supercapacitors for EIS measurements had the same length. h) Cyclic performance of supercapacitor from the CNT/RGO composite fiber. The inset graph showed typical galvanostatic charge–discharge curves at 310 mA cm^{-3}. i) Ragon plot of the supercapacitor fiber based on different carbonaceous fibrous electrodes. Here, OMC and 3D-G represent ordered mesoporous carbon and 3D graphene, respectively.

Figure 2b compares the CV curves of various CNT/RGO composite fibers in H_2SO_4 solution with different deposition times at a scan rate of 50 mV s^{-1}. Their CV curves show reversible cathodic and anodic peaks, suggesting a typical pseudocapacitive behavior. The peaks for 90 s sample were less pronounced because in that condition, GO was less reduced, resulting in a large surface resistance that cannot afford substantial charge transfer.[11] In order to explore the origin of the pseudocapacitance, we conducted the CV tests in a neutral $LiClO_4$ (1 M) electrolyte at the same scanning rates.[15,21] The redox peaks disappeared in the resulting CV curve, indicating that the pseudocapacitance was derived from the remained oxygen-containing functional groups on RGO sheets (Figure S11, Supporting Information).[15] X-ray photoelectron spectroscopy (XPS) analysis revealed that the GO was not completely reduced, which was responsible for the existence of pseudocapacitance (Figure S12, Supporting Information).[22,23]

The specific volumetric capacitance of the composite fibers—calculated by integrating the area of the CV curves—was varied with the increasing electrochemical deposition time (Figure 2c). When the deposition time was less than 180 s, the capacitance was increased with the increasing RGO content. When more RGO was deposited on the interface, the capacitance was decreased. The reason was that the RGO not only introduced pseudocapacitance but also increased the resistance of the electrode (Figure S13, Supporting Information). The high interface resistance was detrimental to the electrochemical performance.[24] In this case, the CNT/RGO composite fiber at an electrochemical deposition time of 180 s exhibited the highest specific volumetric capacitance of 59.8 F cm^{-3}. Note that the volumetric capacitance here refers to the capacitance of a single electrode that is different from the capacitance of a supercapacitor. Therefore, the CNT/RGO composite fibers (180 s) were used for fabricating symmetrical supercapacitors in the following studies.

Based on the electrochemical characterization of CNT/RGO composite fiber, we also investigated the electrochemical performances of the fiber-shaped supercapacitor. Figure 2d shows the CV curves of fiber-shaped supercapacitors based on bare CNT and CNT/RGO composite fibers. The rapid, reversible, and successive surface redox reactions on RGO sheets defined the CV behavior, making the redox peaks indiscernible which is similar to other pseudocapacitive materials like MnO_2.[25] The galvanostatic charge–discharge curves also showed that the capacitance was enhanced by the introduction of RGO layer (Figure S14, Supporting Information). The CV curves of the supercapacitors from this composite fiber can be well maintained under the increasing scan rate from 10 to 500 mV s^{-1}, showing a stable capacitive behavior (Figure S15, Supporting Information). Likewise, the galvanostatic charge–discharge curves of the supercapacitor based on CNT/RGO fiber exhibited a symmetrical shape at various current densities (Figure 2e). The volumetric specific capacitance of the fiber-shaped supercapacitors was calculated from the galvanostatic charge–discharge curves (see Notes in the Supporting Information). The CNT/RGO composite fiber enabled the fiber-shaped supercapacitor a high specific capacitance of 68.4 F cm^{-3} (126.7 F g^{-1}) at 31 mA cm^{-3}, better than the bare CNT fiber supercapacitor (4.5 F cm^{-3} (7.8 F g^{-1}) at 31 mA cm^{-3}). The volumetric capacitances at different current densities indicate that the composite fiber exhibited better electrochemical performances than bare CNT fiber at various current densities, manifesting the decent rate performance (Figure 2f).

The capacitance improvement of CNT/RGO composite fibers can be concluded into several aspects. First, the deposition of RGO significantly improved the hydrophilicity of fibrous electrode (Figure S16, Supporting Information). Because CNTs are hydrophobic (contact angle > 135°), the infiltration of aqueous electrolyte may be impeded by the strong surface tension, yet for the CNT/RGO fiber, the hydrophilic RGO sheets have more affinity for water, rendering larger surface area available for charge storage. Though the specific surface area of RGO sheets and CNT fibers are comparable, the fluorescent microscopic images reveal that the near surface of fibrous electrode mainly contributes to the capacitance (Figure S17, Supporting Information). Therefore, the CNT/RGO composite fiber has a better interface compatibility with gel electrolyte. Second, the oxygen-containing moieties (like carbonyl group and carboxyl group) on the basal plane of RGO provided pseudocapacitance. The pseudocapacitance dominantly contributed to the enhancement of capacitance, which has been demonstrated before and widely reported.[22,23,26] Third, the highly conductive CNT fiber reduced the internal resistance of the fiber-shape supercapacitors, as verified by the electrochemical impedance spectra (EIS) (Figure 2g). The EIS curves of supercapacitors based on different fibrous electrodes exhibit a typical capacitive behavior.[16,27] The horizontal intercept indicates the internal resistance of the supercapacitor. The less-conductive RGO sheets on the surface reduced the conductivity of composite fiber and increased the interface resistance, rendering the larger internal resistance of supercapacitor (Figure S13, Supporting Information). The internal resistance increased with the deposition time which was in line with the IR drop during discharge (Figure S18 and S19, Supporting Information). In contrast, graphene fibers generated the largest internal resistance in supercapacitor due to their inferior conductivity (Figure S20, Supporting Information). Also, at the low frequency region of Figure 2g, the deviation from ideal capacitive behavior can be attributed to the nonuniform microscopic active layer thickness and distribution in charge transfer rates, adsorption processes, or surface roughness.[28]

Figure 2h exhibits the cyclic stability of the fiber-shaped supercapacitors that retained high capacitance during 10 000 charge–discharge cycles. Moreover, the fiber-shaped supercapacitors based on CNT/RGO composite fiber displayed volumetric energy density (E_V) of 2.4 mW h cm^{-3} and areal energy density (E_A) of 3.8 μW h cm^{-2}. The volumetric power density (P_V) and areal power density (P_A) were 0.016 W cm^{-3} and 0.025 mW cm^{-2} at the current density of 31 mA cm^{-3}, respectively. Both energy density and power density were higher than those of previously reported fiber-shaped supercapacitors based on carbon composite fibers (Figure 2i)[9,10] and comparable to the results based on wet-spinning RGO/CNT composite fibers (E_V: 3.5 mW h cm^{-3}, E_A: 3.84 μW h cm^{-2}, P_V: 0.018 W cm^{-3}, and P_A: 0.02 mW cm^{-2}).[16]

Our synchronous deposition strategy was also extendable and transferable to various other pseudocapacitive active materials. It was available to continuously fabricate fiber-shaped supercapacitors with different pseudocapacitive composite fibers. For instance, we used the one-step electrochemical deposition method to continuously prepare CNT/MnO_2 composite fibers for supercapacitors. Scanning electron microscopy (SEM) images show that flower-like MnO_2 particles were anchored on the outer surface of CNT fiber, resulting in a core–sheath-structured CNT/MnO_2 composite fiber (**Figure 3**a). Because of the high conductivity of CNT core and high pseudocapacitance of MnO_2 particles, the electrochemical performances were significantly enhanced as expected (Figure 3b).[12,29] Meanwhile, the galvanostatic charge/discharge curves (Figure 3c) of the resulting supercapacitors showed a symmetrical shape at various current densities, indicating a high reversibility and good charge propagation between the two fiber electrodes. Even at a short deposition time of ≈30 s, the specific capacitance of CNT/MnO_2 composite fiber was increased to 20.2 F cm^{-3} (34.9 F g^{-1}) (about four times higher than the bare CNT fiber), indicating a simple and rapid method to fabricate high-performance supercapacitor fibers.

This method was also compatible for electrochemical polymerization of conductive polymer, which also has high pseudocapacitance as electrode materials in the supercapacitor. As a demonstration, polyaniline (PANI) was continuously deposited on the CNT fiber through synchronous electropolymerization from aniline monomer. Figure 3d shows the SEM images of CNT/PANI composite fiber electrode at different magnifications. The CNT bundles were uniformly coated with a layer of polymer, suggesting that the monomer solution can effectively infiltrate into the inner of CNT fiber before polymerization.[30] The remaining voids in the composite fiber are favorable for the

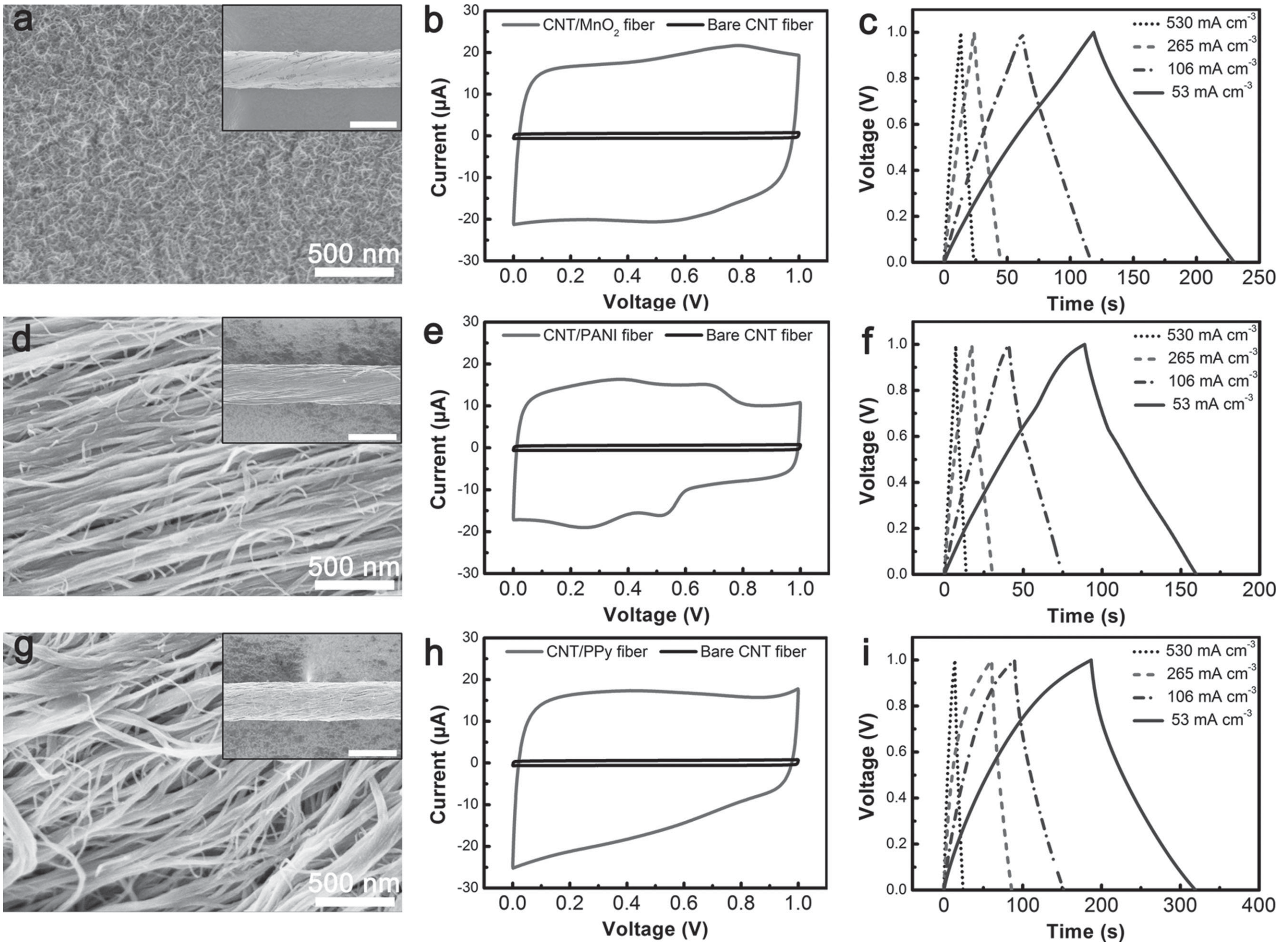

Figure 3. a–c) SEM images, CV curve, and galvanostatic charge–discharge curves of supercapacitor from CNT/MnO$_2$ composite fiber, respectively. d–f) SEM images, CV curve, and galvanostatic charge–discharge curves of supercapacitor from CNT/PANI composite fiber, respectively. g–i) SEM images, CV curve, and galvanostatic charge–discharge curves of supercapacitor from CNT/PPy composite fiber, respectively. The CV curve of bare CNT supercapacitor fiber is compared at (b), (e), and (h). The scanning rate of CV curves in (b), (e), and (h) was the same as 200 mV s^{-1}. Scale bars of the inset of (a), (d), and (g) are 50 μm.

electrochemical performances of fiber-shaped supercapacitors. Electrochemical measurements manifest that these fibrous electrodes delivered high capacitance and stability (Figure 3e,f). Another commonly used conductive polymer polypyrrole (PPy) was also employed as an active material to prepare composite fibers.[31] The electrochemical results showed that the CNT/PPy composite fiber also demonstrated higher performance than the bare CNT fiber (Figure 3g–i). The continuously produced composite fibers exhibited stable electrochemical performances (Figure S21, Supporting Information). Therefore, our one-step electrochemical deposition strategy was reliable and versatile to prepare various high-performance composite fibers.

The flexibility of the fiber-shaped supercapacitors was of great importance to the wearable applications. Here, the composite fibrous electrode inherited the high strength and flexibility of CNT fiber (Figure S22, Supporting Information). The continuous supercapacitor fibers can be arbitrarily bent without structural damage. Dynamic bending test (bent to 180°) during charge and discharge produced almost overlapped galvanostatic charge–discharge curves which exhibited a typical symmetrical shape at increasing bending times (Figure S23, Supporting Information). Furthermore, the fiber-shaped supercapacitor based on different composite fibers preserved more than 95% of its initial capacitance after bending for 1000 cycles (Figure S24, Supporting Information). The microscopic morphologies of the composite fibers after dynamic bending tests exhibit the structural integrity which is indicative of decent endurance to deformations (Figure S25, Supporting Information). Moreover, the above supercapacitor fibers can be connected in series or parallel to control the output voltage or current, respectively (Figure S26, Supporting Information). The continuously produced fiber-shaped supercapacitors had stable performances that were slightly affected by their lengths (Figure S27, Supporting Information). **Figure 4**a shows the knitting process of supercapacitor fibers with cotton fibers through a knitter model. In spite of the existence of mechanical stress, the supercapacitor fibers showed a favorable stitchability, and the fiber structure was well maintained in the knitting process (Figure 4b).

In conclusion, a one-step electrochemical deposition process has been developed to rapidly fabricate continuous fiber-shaped

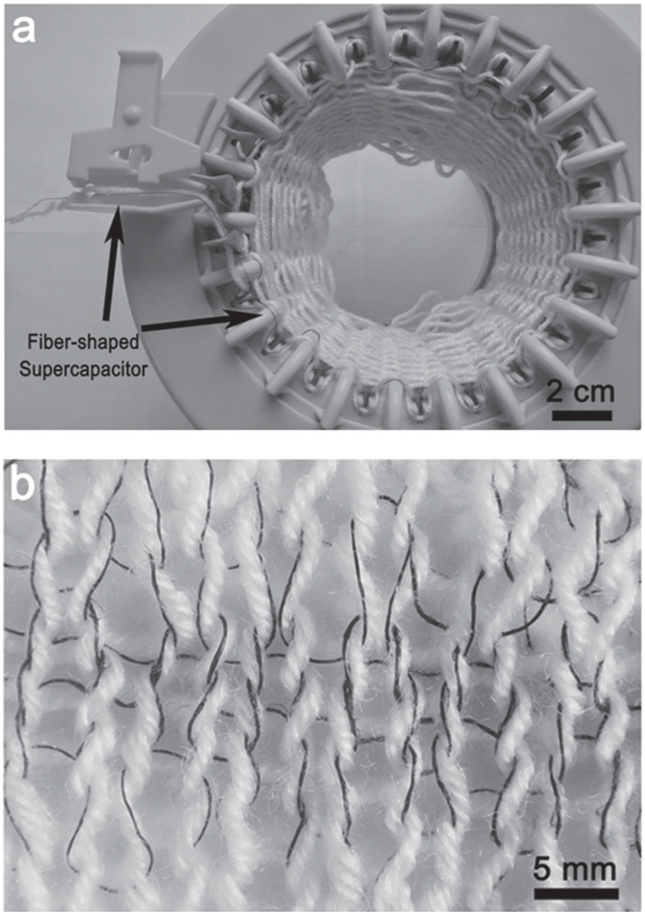

Figure 4. The as-fabricated supercapacitor fiber being woven into flexible textiles. a) Photograph of the knitting process (the arrow showing the inlet of the supercapacitor fiber). b) An integrated fabric woven from cotton yarns (white fibers) and supercapacitor fibers (black fibers).

supercapacitors with a length of 100 cm from primitive CNT array and active materials solution within minutes. This method is simple and highly efficient, and can be easily scaled up for a large production. A variety of pseudocapacitive active materials such as GO, metal oxide, and conductive polymers can be incorporated by the continuous process. Therefore, the resulting all-solid-state supercapacitor fibers show remarkable energy-storage capabilities. This work also presents a general and effective strategy in the development of energy harvesting and storage devices aiming at a large-scale production.

Experimental Section

Fabrication of Supercapacitor from CNT/RGO Composite Fiber: The preparation and experimental setup of the CNT/RGO supercapacitor fiber are schematically shown in Figure 1a. Aligned CNT fibers were first dry-spun from CNT arrays synthesized by chemical vapor deposition.[32,33] The CNT fiber was then passed through the GO solution to produce core–sheath CNT/RGO composite fiber. Here, GO was synthesized from graphite powders by a modified Hummer's method.[34,35] Aqueous GO solution was prepared by dissolving 6 mg GO in 100 mL water, followed by an ultrasonicated treatment for 30 min and addition of 0.1 M $LiClO_4$. Pt wire and Ag/AgCl were used as counter and reference electrodes, respectively. CNT fibers were contacted with two copper rods that were used as current collectors. A constant potential of –1.2 V was then applied on the CNT fibers through the copper rods. The CNT fibers were drawn and collected by the rotating motor and the electrochemical deposition time can be controlled by varying the collecting speed. Polymer gel electrolyte was dip-coated onto the composite fiber to form fibrous electrode. The preparation of polymer gel electrolyte was summarized below. Polyvinyl alcohol (1 g) was added in deionized water (10 mL), followed by stirring at 95 °C for 1 h. After cooling down to room temperature, H_3PO_4 (1 g) was added to the solution, and the mixture was stirred for 2 h. The supercapacitor fiber was finally obtained by twisting two fibrous electrodes together.

Fabrication of Supercapacitors from the Other Composite Fibers: Similar to the fabrication of the CNT/RGO composite fiber, CNT/MnO_2, CNT/PANI, and CNT/PPy composite fibers had been prepared by the same one-step electrochemical deposition method but varying the deposition solution and potential. The deposition solution for CNT/MnO_2 composite fiber consisted of 0.1 M $Mn(CH_3COO)_2$ and 1.0 M Na_2SO_4, and the constant potential was 0.7 V. The deposition solution for CNT/PANI composite fiber consisted of 0.1 M aniline and 1 M H_2SO_4, and the constant potential was 0.75 V. The deposition solution for CNT/PPy composite fibers consisted of 0.1 M pyrrole and 0.1 M KNO_3, and the constant potential was 0.7 V.

Characterization: The structures were characterized by scanning electron microscopy (Hitachi FE-SEM S4800 operated at 1 kV) and Raman spectroscopy (LabRam-1B with excitation wavelength of 633 nm and laser power of 4 mW). Composite fibers were tested in a three-electrode system in 1 M H_2SO_4 aqueous solution (Pt wire and Hg/Hg_2Cl_2 were used as counter and reference electrodes, respectively). Cyclic voltammograms, galvanostatic charge–discharge curves, and electrochemical impedance spectra were recorded in a two-electrode system using an electrochemical analyzer system (CHI 660D).

Supporting Information

Supporting Information is available from the Wiley Online Library or from the author.

Acknowledgements

This work was supported by MOST (2011CB932503), NSFC (21225417, 51403038), STCSM (12nm0503200), China Postdoctoral Science Foundation (2047M560290), the Fok Ying Tong Education Foundation, the Program for Special Appointments of Professors at Shanghai Institutions of Higher Learning, and the Program for Outstanding Young Scholars of the Organization Department of the CPC Central Committee.

Received: July 17, 2015
Revised: August 31, 2015

[1] L. Li, Z. Wu, S. Yuan, X. B. Zhang, *Energy Environ. Sci.* **2014**, *7*, 2101.
[2] X. F. Wang, X. H. Lu, B. Liu, D. Chen, Y. X. Tong, G. Z. Shen, *Adv. Mater.* **2014**, *26*, 4763.
[3] W. Zeng, L. Shu, Q. Li, S. Chen, F. Wang, X. M. Tao, *Adv. Mater.* **2014**, *26*, 5310.
[4] T. Chen, L. B. Qiu, Z. B. Yang, H. S. Peng, *Chem. Soc. Rev.* **2013**, *42*, 5031.
[5] D. S. Yu, Q. H. Qian, L. Wei, W. C. Jiang, K. L. Goh, J. Wei, J. Zhang, Y. Chen, *Chem. Soc. Rev.* **2015**, *44*, 647.
[6] J. A. Lee, M. K. Shin, S. H. Kim, H. U. Cho, G. M. Spinks, G. G. Wallace, M. D. Lima, X. Lepro, M. E. Kozlov, R. H. Baughman, S. J. Kim, *Nat. Commun.* **2013**, *4*, 1970.

[7] G. Z. Sun, J. Q. Liu, X. Zhang, X. W. Wang, H. Li, Y. Yu, W. Huang, H. Zhang, P. Chen, *Angew. Chem., Int. Ed.* **2014**, *53*, 12576.
[8] D. S. Yu, K. L. Goh, Q. Zhang, L. Wei, H. Wang, W. C. Jiang, Y. Chen, *Adv. Mater.* **2014**, *26*, 6790.
[9] J. Ren, W. Y. Bai, G. Z. Guan, Y. Zhang, H. S. Peng, *Adv. Mater.* **2013**, *25*, 5965.
[10] Y. N. Meng, Y. Zhao, C. G. Hu, H. H. Cheng, Y. Hu, Z. P. Zhang, G. Q. Shi, L. T. Qu, *Adv. Mater.* **2013**, *25*, 2326.
[11] Y. Hu, H. H. Cheng, F. Zhao, N. Chen, L. Jiang, Z. H. Feng, L. T. Qu, *Nanoscale* **2014**, *6*, 6448.
[12] C. Choi, J. A. Lee, A. Y. Choi, Y. T. Kim, X. Lepro, M. D. Lima, R. H. Baughman, S. J. Kim, *Adv. Mater.* **2014**, *26*, 2059.
[13] K. Wang, Q. H. Meng, Y. J. Zhang, Z. X. Wei, M. H. Miao, *Adv. Mater.* **2013**, *25*, 1494.
[14] G. Z. Sun, X. Zhang, R. Z. Lin, J. Yang, H. Zhang, P. Chen, *Angew. Chem., Int. Ed.* **2015**, *54*, 4651.
[15] D. S. Yu, K. Goh, H. Wang, L. Wei, W. C. Jiang, Q. Zhang, L. M. Dai, Y. Chen, *Nat. Nanotechnol.* **2014**, *9*, 555.
[16] L. Kou, T. Q. Huang, B. N. Zheng, Y. Han, X. L. Zhao, K. Gopalsamy, H. Y. Sun, C. Gao, *Nat. Commun.* **2014**, *5*, 3754.
[17] H. Sun, X. You, J. E. Deng, X. L. Chen, Z. B. Yang, J. Ren, H. S. Peng, *Adv. Mater.* **2014**, *26*, 2868.
[18] A. V. Neimark, S. Ruetsch, K. G. Kornev, P. I. Ravikovitch, *Nano Lett.* **2003**, *3*, 419.
[19] Y. R. Li, K. X. Sheng, W. J. Yuan, G. Q. Shi, *Chem. Commun.* **2013**, *49*, 291.
[20] X. Fang, Z. B. Yang, L. B. Qiu, H. Sun, S. W. Pan, J. Deng, Y. F. Luo, H. S. Peng, *Adv. Mater.* **2014**, *26*, 1694.
[21] F. Gao, L. Viry, M. Maugey, P. Poulin, N. Mano, *Nat. Commun.* **2010**, *1*, 2.
[22] C.-H. Yang, P.-L. Huang, X.-F. Luo, C.-H. Wang, C. Li, Y.-H. Wu, J.-K. Chang, *ChemSusChem* **2015**, *8*, 1779.
[23] Y. J. Oh, J. J. Yoo, Y. I. Kim, J. K. Yoon, H. N. Yoon, J. H. Kim, S. B. Park, *Electrochim. Acta* **2014**, *116*, 118.
[24] X. D. Zhuang, F. Zhang, D. Q. Wu, X. L. Feng, *Adv. Mater.* **2014**, *26*, 3081.
[25] P. Simon, Y. Gogotsi, *Nat. Mater.* **2008**, *7*, 845.
[26] F. Liu, D. F. Xue, *Chem. Eur. J.* **2013**, *19*, 10716.
[27] X. L. Chen, L. B. Qiu, J. Ren, G. Z. Guan, H. J. Lin, Z. T. Zhang, P. N. Chen, Y. G. Wang, H. S. Peng, *Adv. Mater.* **2013**, *25*, 6436.
[28] R. Kotz, M. Carlen, *Electrochim. Acta* **2000**, *45*, 2483.
[29] J. Ren, L. Li, C. Chen, X. L. Chen, Z. B. Cai, L. B. Qiu, Y. G. Wang, X. R. Zhu, H. S. Peng, *Adv. Mater.* **2013**, *25*, 1155.
[30] Z. B. Cai, L. Li, J. Ren, L. B. Qiu, H. J. Lin, H. S. Peng, *J. Mater. Chem. A* **2013**, *1*, 258.
[31] X. T. Ding, Y. Zhao, C. G. Hu, Y. Hu, Z. L. Dong, N. Chen, Z. P. Zhang, L. T. Qu, *J. Mater. Chem. A* **2014**, *2*, 12355.
[32] T. Chen, L. B. Qiu, H. G. Kia, Z. B. Yang, H. S. Peng, *Adv. Mater.* **2012**, *24*, 4623.
[33] T. Chen, Z. B. Cai, Z. B. Yang, L. Li, X. M. Sun, T. Huang, A. S. Yu, H. G. Kia, H. S. Peng, *Adv. Mater.* **2011**, *23*, 4620.
[34] X. L. Li, H. L. Wang, J. T. Robinson, H. Sanchez, G. Diankov, H. J. Dai, *J. Am. Chem. Soc.* **2009**, *131*, 15939.
[35] J. W. Burress, S. Gadipelli, J. Ford, J. M. Simmons, W. Zhou, T. Yildirim, *Angew. Chem., Int. Ed.* **2010**, *49*, 8902.